Chinese Chemical Letters 34 (2023) 107705

Contents lists available at ScienceDirect

Chinese Chemical Letters

journal homepage: www.elsevier.com/locate/cclet

Janus hydrogel with dual antibacterial and angiogenesis functions for enhanced diabetic wound healing

Guiting Liu[a,1], Yuan Zhou[a,1], Zejun Xu[c], Ziting Bao[c], Li Zheng[d,e,*], Jun Wu[b,c,*]

[a] The State Key Laboratory of Polymer Materials Engineering, Polymer Research Institute of Sichuan University, Chengdu 610065, China
[b] Guangdong Provincial Key Laboratory of Malignant Tumor Epigenetics and Gene Regulation, Sun Yat-sen Memorial Hospital Sun Yat-sen University, Guangzhou 510120, China
[c] School of Biomedical Engineering, Sun Yat-sen University, Guangzhou 510006, China
[d] Guangxi Engineering Center in Biomedical Materials for Tissue and Organ Regeneration, Life Science Institutes, Guangxi Medical University, Nanning 530021, China
[e] Collaborative Innovation Centre of Regenerative Medicine and Medical BioResource Development and Application Co-constructed by the Province and Ministry, Guangxi Medical University, Nanning 530021, China

ARTICLE INFO

Article history:
Received 29 April 2022
Revised 18 July 2022
Accepted 21 July 2022
Available online 23 July 2022

Keywords:
Janus hydrogel
Antibacterial
Angiogenesis
Diabetic wound
Wound healing

ABSTRACT

Anti-infection and neovascularization at the wound site are two vital factors that accelerate diabetic wound healing. However, for a wound healing dressing, the two functions need to work at different sites (inner and outer), giving big challenges for dressing design. In this study, we fabricated a novel sodium alginate/chitosan (SA/CS) Janus hydrogel dressing by the assembly of SA hydrogel loaded with silver nanoparticles (AgNPs) and CS hydrogel impregnated with L-arginine loaded sodium alginate microspheres (ArgMSs) based on electrostatic interactions to combine the two functions. The outer SA-AgNP hydrogel could prevent infection while avoiding the deposition of AgNPs in the wound site, and the inner CS-ArgMS hydrogel on the wound surface could realize the sustained release of L-arginine and promote vascular regeneration. The composition, morphology and swelling/degradation of the SA-AgNP/CS-ArgMS hydrogel were characterized systematically. L-Arginine release behavior has been tested and SA-AgNP/CS-ArgMS hydrogel has been confirmed for excellent biocompatibility. Antibacterial and angiogenesis assays demonstrated the antibacterial and angiogenesis characteristics of the SA-AgNP/CS-ArgMS hydrogel. Finally, *in vivo* diabetic wound healing assay demonstrated that the SA-AgNP/CS-ArgMS hydrogel could significantly accelerate re-epithelialization, granulation tissue formation, collagen deposition and angiogenesis, thereby resulting in enhanced diabetic wound healing

As a severe complication of diabetes, diabetic wounds have already become a substantial threat to human health due to their characteristics of chronic healing and severe body damage, which could result in amputation or even death [1,2]. As reported, there were 463 million diabetic patients worldwide in 2019, and the incidence rate of diabetic ulcers exceeded 6% [3]. The efficient repair of diabetic wounds has been an urgent global challenge [4,5].

Typically, the normal wound healing process can be divided into four overlapping and ordered phases: hemostasis, inflammation, proliferation and remodeling [6]. However, for diabetic wounds, the physiological environment of hyperglycemia disturbs the normal metabolic balance of wound healing, thereby resulting in chronic wounds [7]. Many factors delay the healing of diabetic wounds, among which susceptibility to infection and difficulty of neovascularization in the wound site are two major factors. The hyperglycemic microenvironment of diabetic wounds easily breeds pathogenic bacteria, which causes chronic wound infection and keeps the wound in a state of continuous inflammation [8]. Neovascularization is a critical component of wound healing, which could provide essential nutrition and oxygen for the cells that are involved in wound repair and exclude metabolites during the healing process [9]. However, hyperglycemia hinders vascular regeneration, thereby further leading to diabetic wounds being trapped in the inflammatory state. Therefore, antibacterial and neovascularization are of substantial significance for diabetic wounds to accelerate healing.

Dressing is a common and effective method for treating skin wounds. Hydrogels have been frequently utilized as wound dressings because they can provide a moist environment, simulate the

* Corresponding authors.
E-mail addresses: zhengli224@163.com (L. Zheng), wujun29@mail.sysu.edu.cn (J. Wu).
[1] These authors contributed equally to this work.

https://doi.org/10.1016/j.cclet.2022.07.048
1001-8417/

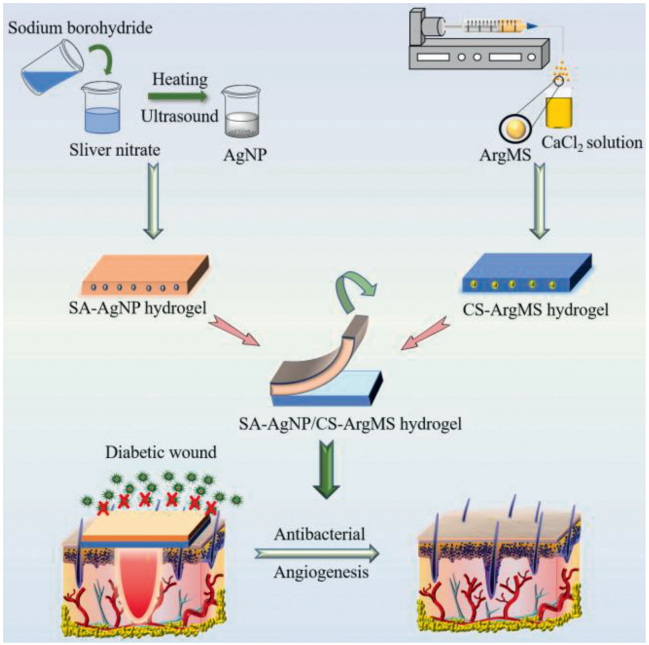

Fig. 1. Schematic diagram of the preparation of the SA-AgNP/CS-ArgMS Janus hydrogel and its mechanism of accelerating diabetic wound healing.

extracellular matrix, and effectively carry bioactive molecules and are easy to utilize at wound sites [10,11]. In the past few years, hydrogels with antibacterial or vascular regeneration functions have gradually emerged. Among numerous antibacterial strategies, silver nanoparticles (AgNPs) have attracted substantial attention due to their high efficiency and broad-spectrum antibacterial properties and their ability to avoid resistance [12]. Nowadays, the utilization of hydrogel dressings that are loaded with AgNPs is a common strategy for preventing the infection of wound sites. For example, Anwarul Hasan *et al.* fabricated chitosan-PEG hydrogel that was impregnated with AgNPs for chronic wound healing applications. The introduction of AgNPs significantly enhanced the antibacterial activity of the hydrogel and had promising applications for diabetic wound treatment [13]. Although AgNPs have fantastic antibacterial activity, a residue of AgNPs in wound sites can severely damage human health [14], which is almost inevitably deposited by hydrogel dressings. Nitric oxide (NO) is a crucial positive regulatory molecule for vascular regeneration [15,16]. However, as the only precursor of endogenous NO in the human body, L-arginine, which could be catalyzed by nitric oxide synthetase to produce NO, is not adequately supplied in diabetic wounds [17]. In contrast to dietary supplementation, the *in-situ* supply of L-arginine to a wound site was found to be a more effective and controllable method for the vascular regeneration of diabetic wounds [18]. However, the sustained release of L-arginine from the hydrogel matrix in the wound site remains a substantial challenge.

Herein, for the first time, we fabricated a novel Janus hydrogel with antibacterial and angiogenesis functions for diabetic wound healing (Fig. 1). Biocompatible polyanionic polysaccharide sodium alginate (SA) and polycation polysaccharide chitosan (CS) were utilized as candidates for the fabrication of Janus hydrogels. An SA hydrogel into which AgNPs had been incorporated *in-situ* functioned as an antibacterial layer, and a CS hydrogel that was impregnated with L-arginine-loaded alginate sodium microspheres (ArgMS) functioned as an L-arginine sustained release layer. An SA-AgNP/CS-ArgMS Janus hydrogel was fabricated *via* the assembly of the SA-AgNP layer and CS-ArgMS layer based on electrostatic interactions. In this design, the outer SA-AgNP hydrogel layer could protect diabetic wounds from bacterial infection while avoiding the deposition of a residue of AgNPs in the wound site. In addition, the ArgMS that was loaded in the CS hydrogel could release L-arginine in a sustained manner due to the electrostatic interaction between L-arginine and the alginate sodium microspheres. Hence, this novel Janus hydrogel platform could provide a simple and practical approach for the fabrication of advanced hydrogel dressings for effective diabetic wound healing.

The preparation of SA-AgNP/CS-ArgMS Janus hydrogel and its physicochemical property characterization were provided in supporting information. Swelling and degradation test, and L-arginine release performance of the hydrogels were carried out. In addition, *in vitro* and *in vivo* tests, including biocompatibility assay, antibacterial assay, angiogenesis assay and diabetic wound healing assay, were performed to evaluate the performance of SA-AgNP/CS-ArgMS Janus hydrogel on promoting diabetic wound healing. All animal protocols in this study were approved by the Animal Care and Use Committee of Sun Yat-sen University. The details of experiment were supplied in supporting information. All experiments were conducted in triplicate, and the experimental data are represented as the mean ± standard deviation (SD). One-way analysis of variance (ANOVA) was conducted to analyze differences among groups, and $^{*}P < 0.05$ indicated statistical significance.

The prepared AgNPs were identified by SEM and XRD (Fig. S1 in Supporting information). SA solutions with various concentrations were used to fabricate SA microspheres to identify the optimal composition. According to Fig. S2 (Supporting information), the hydrodynamic size distribution of the SA microspheres that were prepared with 2 wt% SA solution was the most uniform. Due to the electrostatic interaction, the hydrodynamic size of the SA microspheres could be adjusted *via* the addition of L-arginine. As Fig. S3 (Supporting information) showed, the performance of the ArgMSs that were prepared with 2 wt% SA solution, in which the mass ratio of SA to L-arginine was 2:1, was satisfactorily uniform. Hence, they were suitable for further application. The electrostatic interaction between the SA molecular chain (negatively charged) and L-arginine (positively charged) was demonstrated *via* zeta potential analysis (Fig. S4 in Supporting information). After the introduction of L-arginine, the negative charge on the surface of the SA microspheres was reduced. The composition of ArgMS was identified *via* ATR-FTIR (Fig. S5 in Supporting information). For the alginate microspheres, a peak at 1630 cm^{-1} corresponded to the stretching vibrations of C=O from the –COO– groups of SA. For L-arginine, a peak at 1650 cm^{-1} was attributed to the guanido group, and a peak at 1140 cm^{-1} was assigned to C-C-N asymmetric bending. Due to the embedding and lower content of L-arginine, the FTIR spectrum of ArgMS mainly presented the characteristic absorption peaks of SA. In addition, the morphology of ArgMS was demonstrated *via* TEM (Fig. S5).

The nano-$CaCO_3$/GDL system [19], which can release calcium ions gently at room temperature, is frequently used to prepare SA hydrogels with homogenous structures based on the chelation between calcium ions and the G unit of SA molecules. Genipin, which is a natural biological cross-linker, is often utilized to prepare CS hydrogels at room temperature [20]. In this study, a nano-$CaCO_3$/GDL system and AgNPs were introduced into the SA pre-solution and well mixed. Upon the sustained release of calcium ions *in situ*, the SA-AgNP hydrogel was formed at room temperature. The preparation process of the CS-ArgMS hydrogel was similar. To realize the tight bonding of the SA-AgNP and CS-ArgMS hydrogel layers, an SA-AgNP pre-solution and a CS-ArgMS pre-solution were immediately employed to fabricate SA-AgNP/CS-ArgMS hydrogel using a homemade device after the process of vacuum mixing. The gelation behavior of SA, SA-AgNP, CS and CS-ArgMS pre-solutions were studied by rheological measurements. As presented in Fig. S6 (Supporting information), the introduction

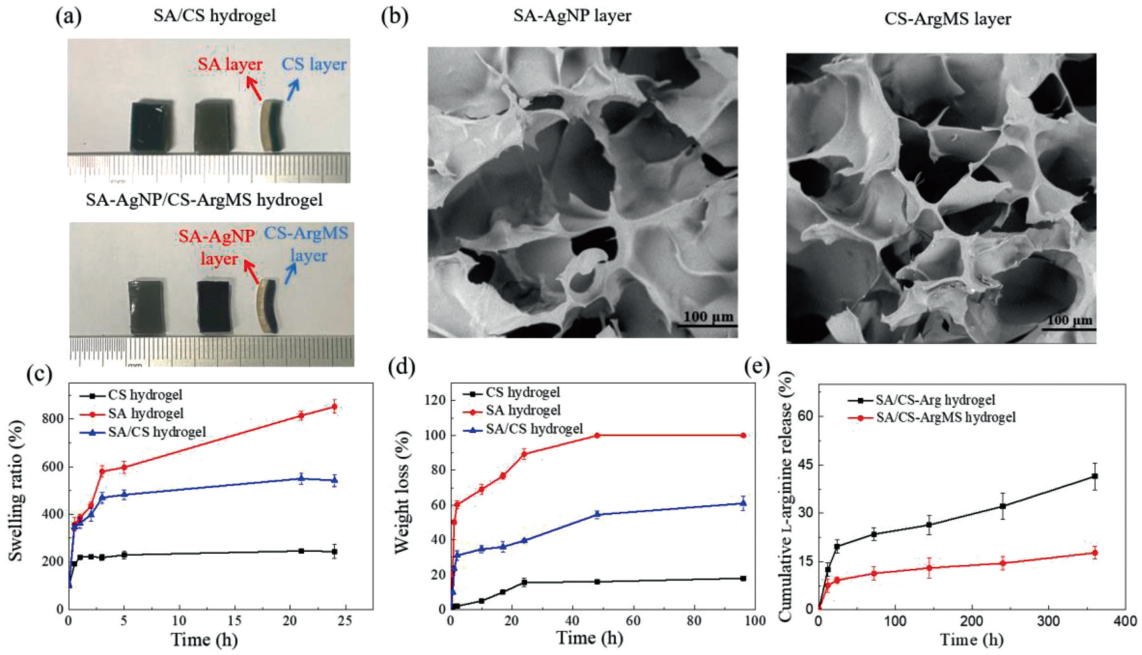

Fig. 2. Macroscopic morphologies of the SA/CS hydrogel and the SA-200AgNP/CS-ArgMS hydrogel (a), SEM images of the SA-ArgNP hydrogel layer and the CS-ArgMS hydrogel layer (b), swelling kinetics (c), degradation kinetics (d) and L-arginine release kinetics (e) of the hydrogels.

of AgNP and ArgMS did not change the gelation time of SA and CS presolutions significantly due to their small amounts. The obtained SA-AgNP/CS-ArgMS hydrogel was presented in Fig. 2a. The SA-AgNP hydrogel layer and the CS-ArgMS hydrogel layer had regular structures, and their interface was clear. In addition, the introduction of AgNPs and ArgMS did not disturb the regularity of the layer structure. According to Fig. 2b, both the SA-AgNP hydrogel layer and the CS-ArgMS hydrogel layer possessed a pore structure, which was beneficial for the transportation of oxygen and the absorption of wound exudation.

Swelling and degradation tests were conducted in a PBS solution at 25 °C. As Fig. 2c shows, the equilibrium swelling ratio of the SA hydrogel (over 800%) substantially exceeded that of the CS hydrogel (approximately 220%), and the equilibrium swelling ratio of the SA/CS hydrogel (approximately 500%) was between those of the SA hydrogel and the CS hydrogel due to the two-layer design. The SA hydrogel was physically cross-linked by calcium ions and could completely degrade in the PBS solution due to substitution between calcium ions and monovalent metal ions, such as K^+ and Na^+. However, the CS hydrogel was chemically cross-linked by genipin and could partially degrade in the PBS solution (approximately 20 wt%, Fig. 2d). Similar to the swelling behavior, the degradation ratio of the SA/CS hydrogel was between those of the SA hydrogel and the CS hydrogel. Nitric oxide (NO) is a crucial positive regulatory molecule for vascular regeneration. However, as the only precursor of endogenous NO in the human body, L-arginine was not adequately supplied in diabetic wounds. Therefore, it was essential to realize the sustained release of L-arginine in diabetic wound sites. The cumulative release profile of L-arginine from hydrogels was presented in Fig. 2e. The results demonstrated that approximately 20 wt% L-arginine was released from the SA/CS-Arg hydrogel in the first 24 h, while the amount that was released from the SA/CS-ArgMS hydrogel was only 10 wt%. A sustained release of L-arginine from the hydrogel matrix could be realized after encapsulation by SA microspheres, which was conducive to diabetic wound healing.

The cell viability of the hydrogels was evaluated by MTT assay (Fig. S7a in Supporting information). The results demonstrated that the NIH-3T3 cell viability exceeded 75% after coculture with the hydrogel extracts for 1 and 3 days; hence, there was no cytotoxicity. After incubation for 3 days, the cell viability of the SA-AgNP/CS-ArgMS hydrogel gradually decreased with increasing AgNP content, which reflected the potential cytotoxicity of the AgNP residue in the wound site. In addition, live/dead staining was conducted for further evaluation. As Fig. S7b (Supporting information) shows, all cells on the surfaces of the hydrogel samples presented a green morphology, which indicated satisfactory cytocompatibility. The hemolysis of the hydrogels was evaluated *via* the direct contact method. The results (Fig. S8 in Supporting information) demonstrated that the hemolysis percentages of all hydrogel samples did not exceed 0.3% and, thus, were far less than the maximum limit (5%); therefore, the blood compatibility was excellent.

Escherichia coli (*E. coli*) and *Staphylococcus aureus* (*S. aureus*) were selected as representative gram-negative bacteria and gram-positive bacteria, respectively. They are among the most common pathogenic bacteria in wound infections. Therefore, they were selected as model bacteria to evaluate the antibacterial properties of the hydrogels. As shown in Fig. 3, due to the presentation of the CS hydrogel [21], the SA/CS hydrogel exhibited antibacterial effects (approximately 30% inhibition for *E. coli* and 35% inhibition for *S. aureus*). With the increase in the AgNP concentration in the SA hydrogel layer, the number of bacterial colony units on the agar plate decreased significantly. For the SA-200AgNP/CS-ArgMS hydrogel, the inhibition rate for *E. coli* exceeded 99.1%, and the inhibition rate for *S. aureus* was approximately 100%, which indicated fantastic antibacterial properties. Furthermore, the *E. coli* growth curve was examined to evaluate the antibacterial properties of the hydrogels. According to Fig. 3d, the *E. coli* growth curve of the SA-200AgNP/CS-ArgMS hydrogel exhibited readily observable hysteresis, and its bacteriostatic time could reach 6–8 h, while for the other hydrogel samples, delayed growth of *E. coli* was not readily observed.

Cell migration is an important factor for angiogenesis in wound sites. A scratch test was conducted to evaluate the impact of hydrogel extracts on NIH-3T3 cell migration (Fig. S9 in Supporting information). At 48 h, the scratch of the SA-200AgNP/CS-ArgMS hy-

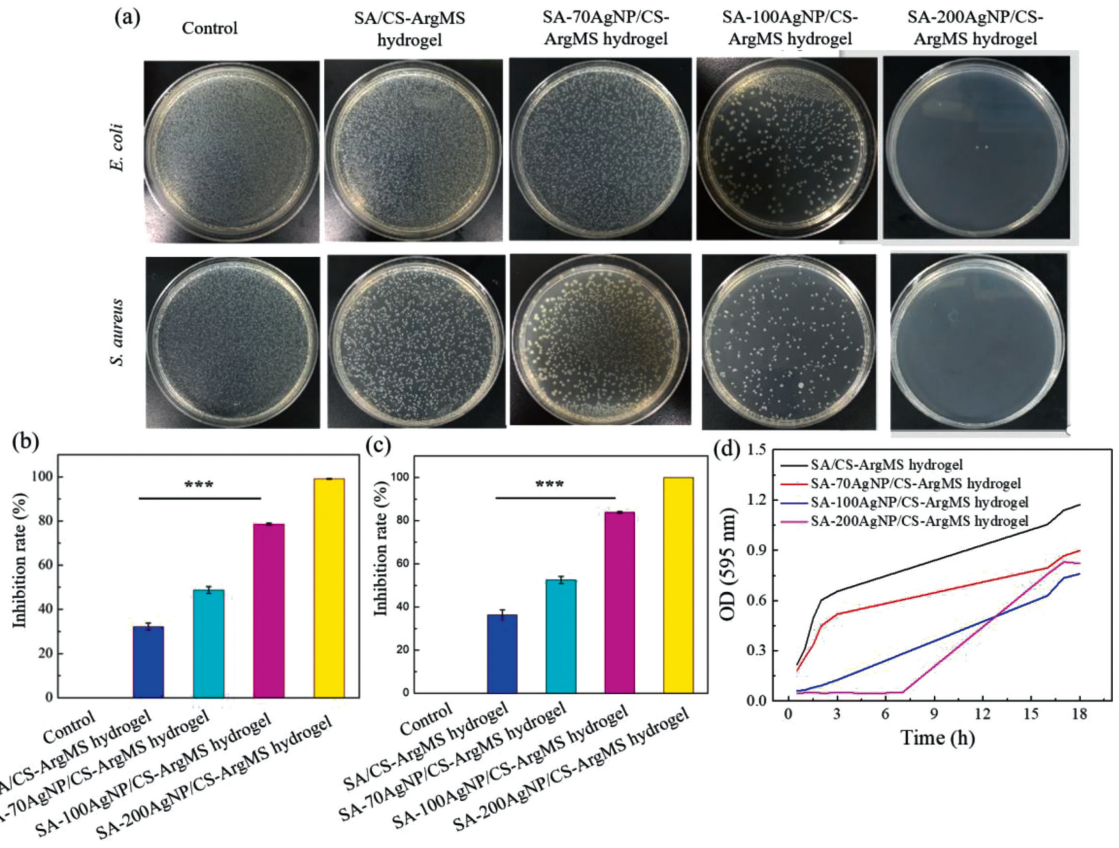

Fig. 3. Inhibitory effects of the hydrogels on *E. coli* and *S. aureus* (a), inhibition rate curves of the hydrogels against *E. coli* (b), inhibition rate curves of the hydrogels against *S. aureus* (c), and growth curves of *E. coli* that was cocultured with the hydrogels (d). $^{***}P < 0.001$.

drogel group almost disappeared, and the healing rate was approximately 90%. Meanwhile, there was still a readily observable gap in the scratch of the SA/CS hydrogel group, with a healing rate of below 80%. At each time point (12, 24 and 48 h), the scratch healing rates of the SA/CS-ArgMS hydrogel and the SA-200AgNP/CS-ArgMS hydrogel significantly exceeded those of the SA/CS hydrogel and the control group, and the rate of the SA/CS hydrogel group also exceeded that of the control group. These results demonstrated that the SA/CS hydrogel platform favored NIH-3T3 cell migration and that the introduction of L-arginine further accelerated cell migration.

The tube formation assay could simulate the process of capillary formation, which was similar to the process in the human body. HUVECs were cultured in a gel matrix to observe whether cells aggregated to form tube-like structures, which could be used to study the angiogenesis-promoting function of samples *in vitro*. According to Fig. S10 (Supporting information), for the SA-200AgNP/CS-ArgMS and SA/CS-ArgMS hydrogels, HUVECs began to form tube-like structures at 2 h, and tube formation was readily observed at 6 h. However, the cells in the control group and the SA/CS hydrogel group were still dispersed and showed no readily observable migration signs and almost no tube-like shapes. The results of both the scratch test and the tube formation assay demonstrated that the introduction of L-arginine could significantly enhance the angiogenesis-promoting function of the SA/CS hydrogel platform.

The above results demonstrated that the SA-AgNP/CS-ArgMS hydrogel, which has both antibacterial and angiogenesis functions and satisfactory biocompatibility, has promising application potential for diabetic wound healing. In this study, a full-thickness diabetic wound model was constructed for evaluating the wound healing activity of the SA-200AgNP/CS-ArgMS hydrogel. Fig. 4 showed images of wounds that were treated with various hydrogel samples at predetermined time points. The closure rate of the wound that was treated with the SA-200AgNP/CS-ArgMS hydrogel was significantly higher than those of the other two groups, and the wound was almost completely closed on the 20th day. In the SA/CS hydrogel group, the wound closure rate exceeded that of the control group due to its hydrogel characteristics of providing a moist environment and simulating the extracellular matrix but was substantially lower than that of the SA-200AgNP/CS-ArgMS hydrogel due to the lack of antibacterial and L-arginine sustained supply functions. In addition, the wound of the control group was slightly suppurative and accompanied by inflammation, while the hydrogel-dressing-treated group had a clean wound surface and no purulent phenomenon occurred. These results demonstrated that the antibacterial and L-arginine sustained supply functions of the hydrogel dressing played highly important roles in the regeneration of diabetic cutaneous wounds.

Furthermore, H&E and Masson's trichrome staining were used to analyze the histological status during wound healing (Fig. S11 in Supporting information). The inflammatory cells in the SA-200AgNP/CS-ArgMS hydrogel group were less infiltrated during the wound healing process. On the 5th day, collagen deposition was readily observed, and on the 10th day, collagen began to differentiate into granulation, with fewer hair follicles and blood vessels. On the 20th day, the granulation tissue structure was satisfactory, and blood vessels were abundant. In addition, collagen fibers were more gathered, intact hair follicles were observed, and the epithelial tissue was completely regenerated, similar to the normal skin. In the CS/SA hydrogel group, on the 5th and 10th days, collagen fibers were produced in small amounts. On the 20th day,

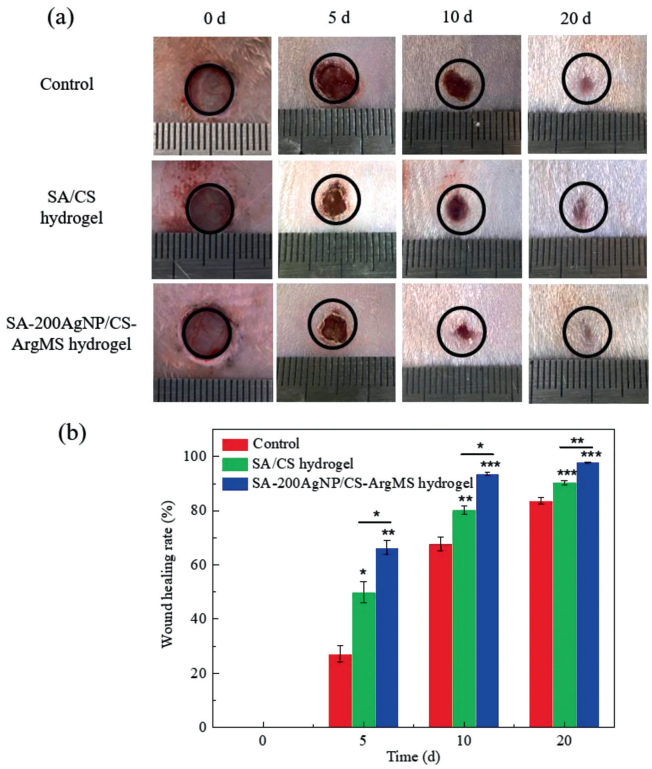

Fig. 4. Representative images of full-thickness excised wounds that were treated with various hydrogels (a) and wound closure rates at various time points (b). $^{*}P < 0.05$, $^{**}P < 0.01$, and $^{***}P < 0.001$.

although the surface was completely healed, only a few hair follicles were observed, and granulation tissue had no readily identifiable structure. In the control group, the wound was substantially infiltrated by inflammatory cells, and on the 20th day, the epithelial tissue was still not fully grown and was in a scabby state, while the granulation tissue had no readily identifiable structure. These results further demonstrated the excellent performance of the SA-AgNP/CS-ArgMS hydrogel for diabetic wound treatment. Immunofluorescence staining of VEGF-A, CD31 and PDGF-B of wound samples at day 20 were further performed to investigate the angiogenic response in diabetic wounds *in vivo*. As presented in Fig. S12 (Supporting information), the SA-200AgNP/CS-ArgMS hydrogel group exhibited the strongest positive expression of the three pro-angiogenic factors, while control group showed very little positive staining. These results indicated that SA-AgNP/CS-ArgMS Janus hydrogel dressing could effectively enhance angiogenesis of diabetic wound, which were consistent with those of H&E and Masson's trichrome staining.

We successfully fabricated a novel SA-AgNP/CS-ArgMS Janus hydrogel for diabetic wound treatment. The outer SA-AgNP hydrogel layer could prevent bacterial infection while avoiding the deposition of a residue of AgNPs in the wound site. Simultaneously, the inner CS-ArgMS hydrogel layer could realize the sustained release of L-arginine and promote vascular regeneration. A biocompatibility assay demonstrated the excellent biocompatibility of the SA-AgNP/CS-ArgMS hydrogel. Furthermore, an *in vivo* diabetic wound healing assay, associating with H&E staining and Masson's trichrome staining, demonstrated that compared with the SA/CS hydrogel and the control group, the SA-200AgNP/CS-ArgMS hydrogel could significantly accelerate re-epithelialization, granulation tissue formation, collagen deposition and angiogenesis, thereby resulting in enhanced diabetic wound healing. This study suggested that this type of Janus hydrogel platform with antibacterial and angiogenesis functions had substantial application potential for diabetic wound treatment.

Declaration of competing interest

The authors declare that they have no known competing financial interests or personal relationships that could have appeared to influence the work reported in this paper.

Acknowledgments

This work was supported by National Natural Science Foundation of China (Nos. 51973243 and 52103039), General Program of Guangdong Natural Science Foundation (No. 2020A1515010983), Science and Technology Planning Project of Shenzhen (No. JCYJ20190807155801657).

Supplementary materials

Supplementary material associated with this article can be found, in the online version, at doi:10.1016/j.cclet.2022.07.048.

References

[1] G. Ceilley, Adv. Ther. 34 (2017) 599–610.
[2] G. Liu, Z. Bao, J. Wu, Chin. Chem. Lett. 31 (2020) 1817–1821.
[3] B. Lya, C. Psa, D. Mra, et al., Diabetes Res. Clin. Prac. 157 (2019) 107841.
[4] L.P. Yuan, M. Pan, K. Shi, et al., Appl. Mater. Today 27 (2022) 101438.
[5] G. Chen, Y. Yu, X. Wu, et al., Research 2019 (2019) 6175398.
[6] C. Xian, Z. Gu, G. Liu, J. Wu, Chin. Chem. Lett. 31 (2020) 1612–1615.
[7] C.H. Su, W.P. Li, L.C. Tsao, et al., ACS Nano 13 (2019) 4290–4301.
[8] S. Wang, H. Zheng, L. Zhou, F. Cheng, Q. Zhang, Nano Lett. 20 (2020) 5149–5185.
[9] M. Wang, C. Wang, M. Chen, Y. Xi, B. Lei, ACS Nano 13 (2019) 10279–10293.
[10] D. Stern, H. Cui, Adv. Healthc. Mater. 8 (2019) 1900104.
[11] Z. Bao, Z. Gu, J. Xu, M. Zhao, G. Liu, J. Wu, Chem. Eng. J. 396 (2020) 125353.
[12] K. Kalantari, E. Mostafavi, A.M. Afifi, et al., Nanoscale 12 (2020) 2268–2291.
[13] N. Masood, A. Rashid, T. Muhammad, et al., Int. J. Pharm. 559 (2019) 23–36.
[14] R.J. Griffitt, C.M. Lavelle, A.S. Kane, N.D. Denslow, D.S. Barber, Aquat. Toxicol. 130–131 (2013) 192–200.
[15] J. Hou, Y. Pan, D. Zhu, et al., Nat. Chem. Biol. 15 (2019) 151.
[16] X. Zhou, H. Wang, J. Zhang, et al., Acta Biomater. 54 (2017) 128–137.
[17] E. Hou, N. Sun, F. Zhang, et al., Cell Rep. 19 (2017) 1631–1639.
[18] M.J. Malone-Povolny, S.E. Maloney, M.H. Schoenfisch, Adv. Healthc. Mater. 8 (2019) 1801210.
[19] J. Yan, Y. Miao, H. Tan, et al., Mater. Sci. Eng. C 63 (2016) 274–284.
[20] J. Yu, Y. Zhang, J. Wang, et al., Nano Res. 12 (2019) 1539–1545.
[21] H.K. No, N.Y. Park, S.H. Lee, S.P. Meyers, Int. J. Food Microbiol. 74 (2002) 65–72.